

Monte-Carlo study of scaling exponents of rough surfaces and correlated percolation

I. Mandre and J. Kalda

Institute of Cybernetics at Tallinn University of Technology, Akadeemia tee 21, 12618, Tallinn, Estonia

We calculate the scaling exponents of the two-dimensional correlated percolation cluster's hull and unscreened perimeter. Correlations are introduced through an underlying correlated random potential, which is used to define the state of bonds of a two-dimensional bond percolation model. Monte-Carlo simulations are run and the values of the scaling exponents are determined as functions of the Hurst exponent H in the range $-0.75 \leq H \leq 1$. The results confirm the conjectures of earlier studies.

I. INTRODUCTION

The world around us is chaotic and seemingly random, but one can still find regularities. Take mountain ranges — these irregular jagged structures may seem intractable to analysis, but often display an interesting property — they look the same at different length scales — they are self-similar. This phenomenon is not limited to the surface features of planets, but is also found in many other places — deposited metal films [3], ripple-wave turbulence [4], crack fronts in material science [5–7], cloud perimeters [8], passive tracers in two-dimensional fluid flows [9–12], etc.

The analysis of these physical systems is often reduced to determining the scaling exponents characterizing the rough surfaces involved. For example, the convective-diffusive transport of a passive scalar in a random two-dimensional steady flow is determined by the scaling exponent of the isolines of the underlying stream-function [11].

The aim of this paper is to numerically calculate the values of these exponents depending on the roughness parameter H . In Sec. II, we start off by giving an overview of the concepts used — rough surfaces and percolation

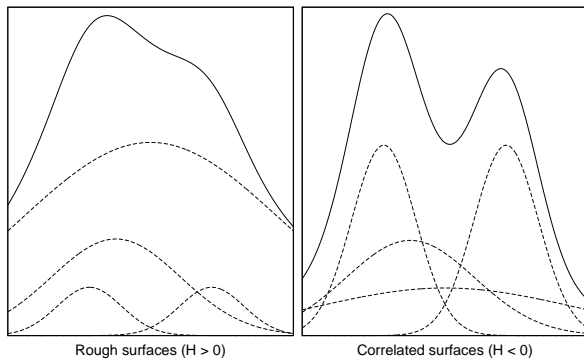


Figure 1: The potential (4) is made up of components with different amplitudes. The amplitude of a component of scale λ is proportional to λ^H . For $H > 0$ the wider “hills” start to dominate the landscape and once $H \geq 1$ only the widest “hill” matters. Conversely, for $H < 0$ local fluctuations start to gain in influence and once $H < -0.75$ the wider hills lose any influence on the scaling exponents of the surface.

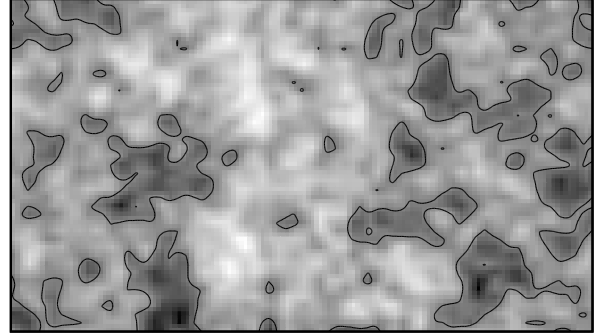


Figure 2: An example of a random potential ($H = 0$ and so $D_h = 1.5$ [1, 2]) with isolines separating the area into “land” and “sea”.

clusters, what we mean by correlations, and a mapping between the two classes of models. Numeric calculations are done through the Monte-Carlo simulations using the two-dimensional bond percolation model; the procedure is described in Sec. III. Interpretation of the resulting data requires overcoming the finite size effects and the convergence problems, which is the subject of Sec. IV. Finally, Sec. V provides a brief summary of the results and a future outlook for the studies of the statistical topography of random surfaces.

II. OVERVIEW

Rough surfaces. Let $\psi(x, y) \equiv \psi(\mathbf{r})$ be the height or potential of a self-similar random two-dimensional surface. We define the roughness exponent H — also known as the Hurst exponent — through the surface height drop at distance $a = |\mathbf{a}|$ [13]:

$$\langle [\psi(\mathbf{r}) - \psi(\mathbf{r} + \mathbf{a})]^2 \rangle \propto |\mathbf{a}|^{2H}, \quad (1)$$

where angular braces denote averaging over the coordinate \mathbf{r} (or also over an ensemble of surfaces). This scaling law assumes that $a_0 \leq |\mathbf{a}| \leq a_1$, where a_0 and a_1 are the lower and upper cut-off scales, and $0 \leq H \leq 1$. Relation (1) also describes self-similarity — the height of a “hill” on the surface is a power law of its diameter, so hills at different scales have the same proportions.

A more generic description, which is not limited to the positive values of H , can be given through the power spectrum $P_{\mathbf{k}}$ [14]. We assume that

$$\langle \psi_{\mathbf{k}} \rangle = 0, \quad \langle \psi_{\mathbf{k}} \psi_{\mathbf{k}'} \rangle = P_{\mathbf{k}} \delta_{\mathbf{k}+\mathbf{k}'}, \quad (2)$$

and define the spectral density $P_{\mathbf{k}}$ as a power law:

$$P_{\mathbf{k}} \propto |\mathbf{k}|^{-2H-2}, \quad \text{for } |\mathbf{k}| \ll a_0^{-1}. \quad (3)$$

This also allows us to conveniently divide the “multiscale” potential $\psi(\mathbf{r})$ into a sum of “monoscale” functions,

$$\psi(\mathbf{r}) = \sum_{\lambda_i=2^i \lambda_0} \psi_{\lambda_i}(\mathbf{r}), \quad (4)$$

where each component in the sum represents a function with a single characteristic length. The effect of the parameter H on the amplitude of the “monoscale” components of the “multiscale” potential can be seen in Fig. 1.

The potential ψ can be also characterized through a correlation function (covariance)

$$C(\mathbf{a}) = \langle \psi(\mathbf{x}) \rangle \langle \psi(\mathbf{x} + \mathbf{a}) \rangle. \quad (5)$$

Indeed, for potentials conforming to (3), it is a power law

$$C(\mathbf{a}) \propto |\mathbf{a}|^{2H} \quad a_0 \ll |\mathbf{a}| \ll a_1, \quad (6)$$

which is valid for the range $-3/4 \leq H \leq 1$.

With a specific height h , the random potential defines a set of isolines $\psi(\mathbf{r}) = h$ (see Fig. 2 for an example). The height h can be interpreted as the “sea level”. So, a single isoline can be looked at as the coastline of an island or a lake. The coastline is also a self-similar structure, and one can quickly run into difficulties when trying to measure its length — the result depends on the size of the measuring stick used [15]. The parameter that best characterizes isolines is their scaling exponent — also called their fractal dimension D_h — which is a fractional number. The length of a coastline can then be given through

$$\langle L(\lambda) \rangle \propto \lambda^{1-D_h}, \quad (7)$$

where λ is the size of the measuring stick. D_h is a nontrivial function of the underlying surface’s Hurst exponent:

$$D_h = D_h(H). \quad (8)$$

Alternatively, we can take two points at a distance a on a coastline, and calculate the length of the line between them, assuming a fixed measuring stick $\lambda = \lambda_0$:

$$\langle L(a) \rangle \propto a^{D_h}. \quad (9)$$

The percolation problem is concerned with the structures that form by randomly placing elementary geometrical objects (spheres, sticks, sites, bonds, etc.) either freely into continuum, or into a fixed lattice (Fig. 3). Two objects are said to communicate, if their distance is less than some given λ_0 , and communicating objects

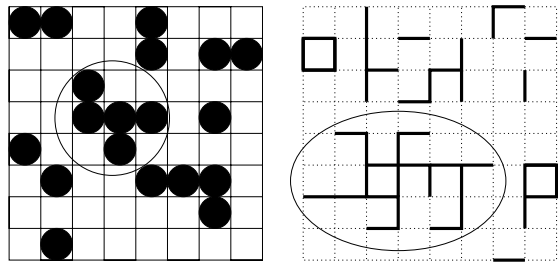


Figure 3: Examples of regular percolation lattices. Square lattice site model to the left and square lattice bond model to the right. Largest clusters have been circled.

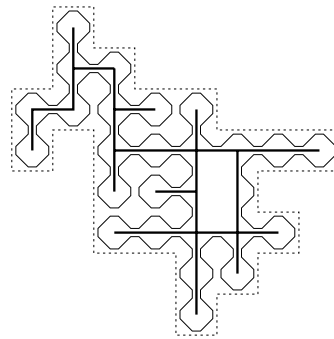


Figure 4: An example square bond percolation cluster. The cluster is made up of the bold segments, the zig-zag is the hull and the dashed line is the unscreened perimeter.

form bigger structures called clusters. Percolation theory studies the formation of clusters and their properties. The more interesting aspect is when and how is an infinite cluster formed. This depends on the lattice site occupation probability η . The minimum site occupation probability when an infinite cluster appears is called the percolation threshold η_c . Near this probability, the percolation model displays a critical behavior and long-range correlations.

Percolation theory is used to study and model a wide variety of phenomena: from a fluid flow in a porous medium to thermal phase transitions and critical behavior in magnetism with dilute Ising models.

The structures that can be identified in conjunction with a percolation cluster are the cluster itself, the hull and the unscreened perimeter (Fig. 4). Aside from these one more structure can be identified — the oceanic coastline [16]. It is comprised of the hull of a cluster and also the hulls of all the holes (reverse clusters) within it. Near the percolation threshold, all of these structures (the cluster, the hull, the unscreened perimeter and the oceanic coastline) are fractals and can be characterized by scaling exponents.

Looking at a percolation cluster and an isoline of a random potential, we can identify similar structures: one can look at the percolation cluster as an island and its hull as the coastline of the island. This idea will be fleshed out

in more precise terms farther below, where a mapping between the two models is described.

One very important and useful aspect about the scaling exponents is a phenomenon known as universality [14] — within specific universality classes, the scaling exponents take the same value across different percolation models. More specifically, they are invariant to small fluctuations or distortions in the lattice structure (for instance, decaying exponentially to distance). This means that the scaling exponents for both the random square bond lattice, and the random square site lattice are the same: the both models belong to the same universality class of the two-dimensional uncorrelated percolation.

Correlated percolation. Percolation lattice does not need to be completely random, but can entail certain correlations. Here we describe the percolation lattice through an infinite set of random variables θ_i which are unity at occupied sites and zero at empty sites (i denotes the site number). Then we can characterize the correlations through the correlation function

$$c_\theta(\mathbf{x}_i - \mathbf{x}_j) = \langle \theta_i \theta_j \rangle - p^2, \quad (10)$$

where $p = \langle \theta_i \rangle$ is the site occupation probability.

Alternatively [17], correlations can be brought into the percolation model by assigning each lattice site a random number $p_i \in [0, 1]$ where $\langle p_i \rangle = p$. The site values are then calculated as

$$\theta_i = \Theta(p_i - x_i), \quad (11)$$

where $\Theta(x)$ is the Heaviside step function and $\{x_i\}$ are independent random variables uniformly distributed in $[0, 1]$. The correlation function is

$$c_p(\mathbf{x}_i - \mathbf{x}_j) = \langle p_i p_j \rangle - p^2 \quad (12)$$

and $c_\theta(\mathbf{a}) = c_p(\mathbf{a}) = c(\mathbf{a})$ [14].

We are interested in algebraically decaying correlations so that

$$c(\mathbf{a}) \propto |\mathbf{a}|^{2H}, \quad H \leq 0. \quad (13)$$

It is believed [14] that the universality class is determined by the two-point correlation function. One can show that at $H < -3/4$, the model belongs to the universality class of uncorrelated percolation [17]. However, in the range $-3/4 \leq H \leq 0$, the correlations do affect the scaling exponents.

There exists a simple mapping between the rough surfaces and the percolation model [18, 19]. According to it, the local maxima of the potential define the lattice sites and the lattice bonds are obtained by drawing fastest-ascent paths from all the saddle points (Fig. 5). The surface $\psi(\mathbf{x})$ is “flooded” at a given level h and a bond i is left connecting if the saddle point \mathbf{x}_i on it is above the water (is land), that is when $\psi(\mathbf{x}_i) \geq h$. As a result, we get an irregular two-dimensional lattice; recall that as per universality, small distortions of the lattice don’t affect the resulting scaling exponents. With this

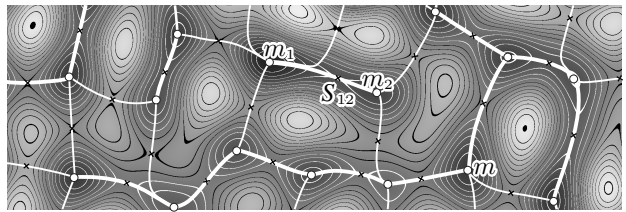


Figure 5: Mapping between the random surfaces and the percolation problem. The bond between two maxima m_1 and m_2 is connecting, if the saddle point S_{12} on them is above the flood level. So, saddle points are mapped into percolation bonds.

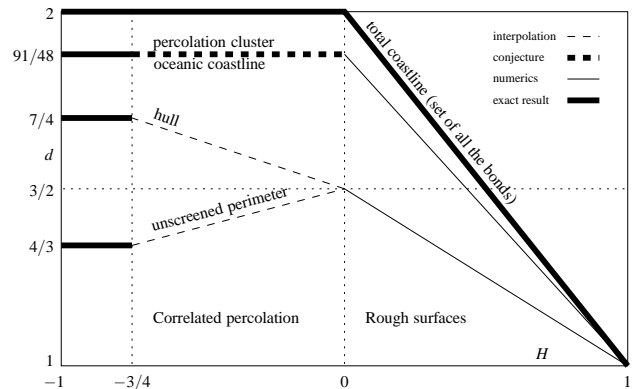


Figure 6: Known results, conjectures and interpolations for the scaling exponents as functions of the Hurst exponent H . While these functions can be approximated as linear functions, they are in fact non-trivial.

mapping, we can relate the islands formed at flooding to the resulting clusters, and their coastlines to the hulls of the said clusters. Also, if the surface correlation function (5) is a power law (6), then so is the correlation function (10) for the percolation model (13), where the parameter H is the same. Due to universality, the scaling exponents of the matching structures are also the same.

The scaling exponents are of interest in many applications so, there is a need to calculate their values depending on the underlying surface’s roughness parameter H . In Fig. 6, we can see the known results (numeric and analytic), and also interpolations and conjectures for the range $-3/4 \leq H \leq 0$. Our next task is to run simulations to numerically shed light on these gray areas (the scaling exponents of the hull and the unscreened perimeter). As these exponents behave the same way for the both problems of rough surfaces and correlated percolation, we can calculate them using the model which is the most convenient from the numerical point of view.

III. MONTE-CARLO SIMULATIONS

Generation of percolation clusters. We calculate the scaling exponents using the model of correlated two-

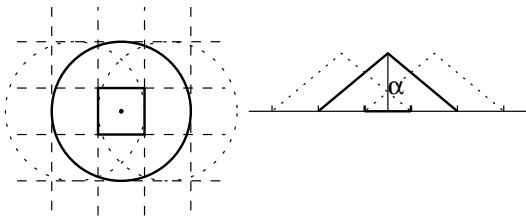


Figure 7: For the i -th layer $\psi_{\lambda_i}(\mathbf{r})$ in (4), we divide space into a grid of cells with side length of $\lambda_i = 2^i$ ($\lambda_0 = 1$). At the center of each cell j , a cone is placed with height $\alpha_j = r_j 2^{iH}$, where r_j is an independent uniform random variable in the range $[-0.5, 0.5]$. The cones have a diameter of $3\lambda_i$ and so overlap.

dimensional bond percolation on square lattices. Our first task is to generate said percolation models so that they conform to the correlation function (13). For this, we first generate random potentials with the requested roughness H . We take the “flood level” as the value of the potential at some starting location \mathbf{x}_0 , so that $h = \psi(\mathbf{x}_0)$, and use it to map the random surface model into one of the percolation models. This is done by overlaying the percolation lattice on the rough surface and calculating the bond values using the Heaviside step function as

$$\theta_i = \Theta(\psi(\mathbf{x}_i) - \psi(\mathbf{x}_0)). \quad (14)$$

This approach is similar to the one described by equation (11) and preserves the correlation exponent. It is slightly different from the maxima-saddle point mapping, but due to universality, there will be no change in the values of the scaling exponents. Using the potential as the underlying model allows us to get the results in the parameter range $-0.75 \leq H \leq 1$.

To generate random potentials, we exploit formula (4). We generate different components (layers) of the potential for different lengths and sum them up. The i -th layer $\psi_{\lambda_i}(\mathbf{r})$ is formed by a grid of cells, where the grid cell side length is 2^i , and at the center of each cell j we place a cone of height $r_j 2^{iH}$, where r_j is an independent uniform random variable in the range $[-0.5, 0.5]$ (Fig. 7). The cones have a diameter of $3\lambda_i$, so the resulting overlap yields a smoother potential. However, the overlap or the shape used (cone, in this case) does not significantly affect how fast the results converge to the asymptotic power laws. So, one can choose a shape more optimized for the speed of numerical calculations (for instance, one could use a simple block or a cylinder). The number of layers required depends on the value of H . For example, at $H = 0$, we can work with $i = 0 \dots 30$.

Gathering data is a matter of generating percolation clusters of different sizes and tracing the structures of interest within these. For the hull, this is done in the following way. We constrain ourselves to a $a \times a$ box, and start to dynamically trace the hull from the center point \mathbf{x}_0 until it reaches any sides of the box (Fig. 8). Hulls that make a full circle are discarded. To get additional data, we also trace backwards from the center,

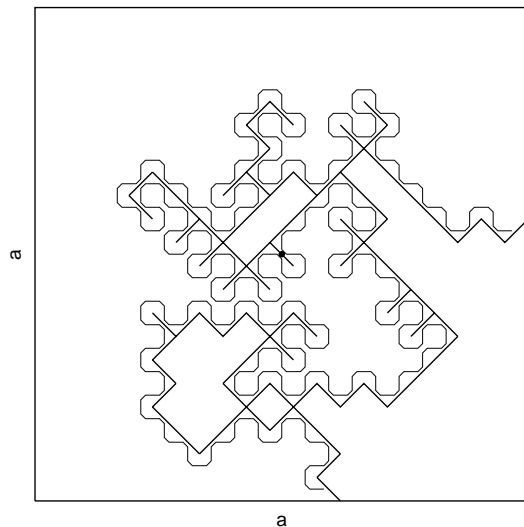


Figure 8: Calculating the length of a hull for size a . We start from the center of a $a \times a$ box and dynamically calculate bond values as we trace the hull until reaching the side of the box. We discard hulls that make a full circle. The box sizes picked are $a = 8, 16, 32, \dots, 1024, \dots$

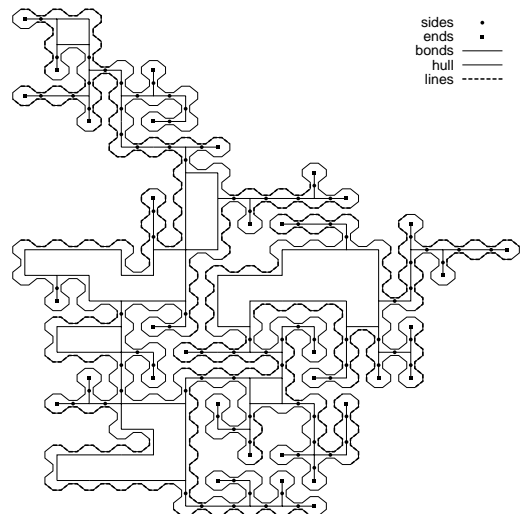


Figure 9: Counting the size of the hull can be done in many ways. One can simply count the number of segments (hull), the number of bonds the hull touches from both sides (sides), the total number of bounds the hull touches (bonds), the number of times a single bond sticks out (ends), or the number of times the hull forms a straight line of 4 segments (lines). All of these scale with the same power law.

so that the both ends of the hull reach the box’s sides. We do this millions of times for differently sized boxes $a = 8, 16, \dots, 1024, \dots$. While for some cases, the range of values $a = 8, 16, \dots, 512$ is sufficient, slow convergence in some regions of H forces us to use larger lattices. However, the size is limited by computational resources and in our case it was not practical to go over $a = 2048$.

Once we have a hull, we want to measure its size

(length). While the easiest way would be to just sum the number of segments in the trace line, it is also possible to determine the size by other properties (Fig. 9). All of these properties scale with the same power law. We can denote the size of a single hull as $L_i(a_j)$, where i indicates the property. As this is different for each individual hull, we find the average value

$$\mathcal{L}_i(a_j) = \langle L_i(a_j) \rangle, \quad (15)$$

and as per equation (9), this should scale as a power law with the exponent D_h . However, the scaling is asymptotic ($a \rightarrow \infty$), so for finite a , there are sizable deviations called finite size effects. These come from the geometry and finite size of the lattice. Using (9), we can estimate the exponent as

$$\tilde{D}_h(\sqrt{a_j a_{j-1}}) \simeq \ln_2 \frac{\mathcal{L}(a_j)}{\mathcal{L}(a_{j-1})} \quad (a_j = 2a_{j-1}). \quad (16)$$

Plotting this for the uncorrelated percolation (Fig. 10), we can see how the different properties converge towards the value $D_h = 7/4$. The finite size effects are strongly manifested for the smaller lattices.

IV. DATA ANALYSIS

To calculate the scaling exponents from the data, the following assumptions are made:

1. the mathematical expectation for each property can be described as an infinite series

$$\bar{L}_i(a) = \sum_{\mu=1}^{\infty} A_{i\mu} a^{\alpha_{i\mu}}, \quad \alpha_{i(\mu+1)} < \alpha_{i\mu}, \quad (17)$$

where $i = 1, \dots, m$;

2. $\alpha_{i\mu} \equiv \alpha_\mu$ for $\mu = 1, \dots, m$;
3. the leading terms in the sum are linearly independent ($\det \|A_{\mu i}\| \neq 0$).

After these assumptions, we apply a variation of the least squares method described in [20] and previously used in [16]. The method works if the assumptions made are correct (the method also validates them) and yields us the value α_1 , which is the scaling exponent we are looking for. So, the reason why we counted all the different properties for the hull (Fig. 9), is that they are necessary for this method.

For the unscreened perimeter, a similar approach is taken. The unscreened perimeter is obtained by taking a hull but pruning it from “fjords”.

Convergence problems. In some areas the calculations are hindered by very slow convergence. Let parameter S represent the length at which the covariance of the generated potential starts to differ from that of the ideal $|\mathbf{a}|^{2H}$ law:

$$S = 3 \cdot 2^{s-1}, \quad (18)$$

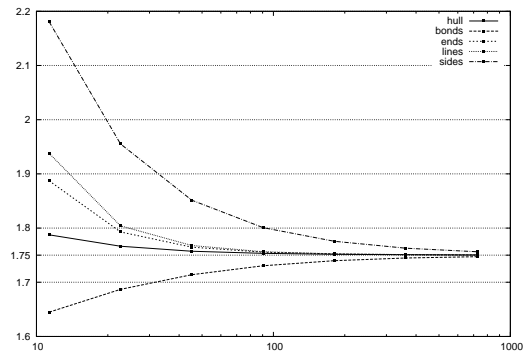


Figure 10: Convergence of the hull properties for the uncorrelated percolation (towards $D_h = 7/4 = 1.75$).

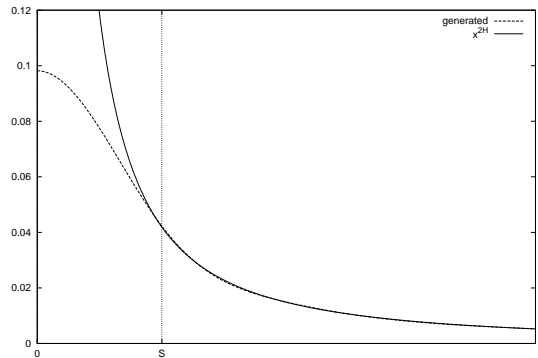


Figure 11: Covariance of a potential versus the power law x^{2H} . Here S marks the length at which the covariance starts to diverge from the power law.

where s indicates the smallest-scale layer index (Fig. 11). When S decreases (by adding bottom layers), local fluctuations start to gain in influence compared to those of the long-range correlations. This causes a strong finite-size effect and the scaling exponents behave as if H was smaller (Fig. 12). Conversely, when increasing S , the scaling exponents can initially behave as if H was greater than it really is.

To get over these distortions, one could calculate for bigger lattice sizes. But often this is not an option as convergence can be very slow and computational resources are limited. Another way would be to manually find the optimal layer configuration that minimizes distortions. This is the approach we took and yielded good results for the hull (aside from the values $H = -0.75$ and $H = +1.00$). However, the convergence of the unscreened perimeter is very sensitive to changes in the layer configuration and for most data points did not yield clear results.

The results can be seen in Fig. 13 and Tab. I. The hull behaves as expected. While it did not yield clear results at $H = -0.75$ and $H = 1.00$, the extrapolations provided seem to indicate that it terminates at $7/4$ and 1 respectively. Due to the convergence problems, the re-

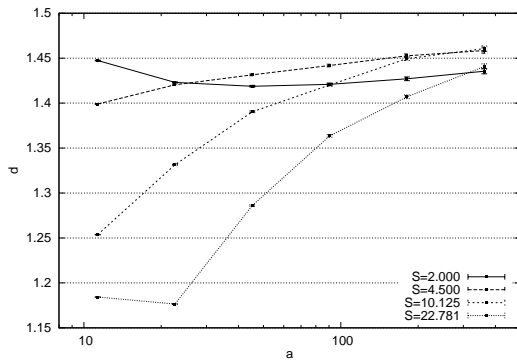


Figure 12: Convergence of a property of the unscreened perimeter at $H = 0$ (towards theoretically known $D_u = 1.5$) for different values of parameter S .

sults for the unscreened perimeter are not as clear. However, one can say that at least that the result do not contradict the analytical findings and support the applicability of a nearly-linear interpolation between the points $D_u(0) = 1.5$ and $D_u(-3/4) = 4/3$.

V. CONCLUSION

We have run Monte-Carlo simulations to determine the scaling exponents of the hull and the unscreened perimeter as functions of the Hurst exponent in the range $-0.75 \leq H \leq 1$. For this, we first generated random potentials conforming to the required correlation function by summation of component potentials of different characteristic lengths and mapping the potential into percolation models. Hulls and unscreened perimeters were traced from these models, and their lengths calculated for different scales. A variation of the least squares method was used to obtain the values of the exponents.

The results confirm the previously known data in the

range $0 \leq H \leq 1$ and also the conjectures for the behavior in the range $-0.75 \leq H \leq 0$, see Fig. 13. The particular results regarding the fractal dimension $D_h(H)$ of hulls confirm that for $0 \leq H \leq 1$, the 4-vertex model (i.e. the rough surfaces in 1+1-dimensional geometry) [21] belongs to the same universality class as the isotropic Gaussian self-affine surfaces (assuming the respective equality of the Hurst exponents). Indeed, comparing the numerical results of Ref. [21] and those of the current study shows that for the entire range of $0 \leq H \leq 1$, the values of $D_h(H)$ coincide within the uncertainties of $ca 10^{-3}$. An important consequence is that the conjecture about the super-universality of the loop correlation exponent $x_l(H) \equiv \frac{1}{2}$ [1, 2] (which has been exploited in several studies, c.f. [22–25]) is clearly rejected: this conjecture implies $D_h(H) = \frac{3}{2} - \frac{H}{2}$, which falls well beyond the uncertainty margins of the present simulation results (for instance, at $H = \frac{1}{2}$, the conjectured value $\frac{5}{4}$ falls far from the range of 1.2820 ± 0.0008).

The obtained results are valuable for a range of practical applications (such as the turbulent transport in quasi-stationary velocity fields), for which the scaling exponents have been analytically expressed via the fractal dimension of the hull. As a future outlook, our method can be applied to calculate other scaling exponents of the correlated percolation problem and statistical topography, such as the fractal dimensions of the clusters (oceanic coastlines), percolation backbone, etc. It can be also extended to study the scaling laws of the transport on quasi-stationary velocity fields.

VI. ACKNOWLEDGMENTS

This work was supported by Estonian Science Targeted Project No. SF0140077s08 and Estonian Science Foundation Grant No. 7909.

-
- [1] J. Kondev and C. L. Henley, *Physical Review Letters* **74**, 4580 (1995).
 - [2] J. Kondev, C. L. Henley, and D. G. Salinas, *Physical Review E* **61**, 104 (2000).
 - [3] G. Palasantzas and J. Krim, *Physical Review Letters* **73**, 3564 (1994).
 - [4] W. B. Wright, *Science* **278**, 1609 (1997).
 - [5] E. Bouchaud, G. Lapasset, J. Planès, and S. Naveos, *Physical Review B* **48**, 2917 (1993).
 - [6] S. Santucci, K. Måløy, A. Delaplace, J. Mathiesen, A. Hansen, J. Haavig Bakke, J. Schmittbuhl, L. Vanel, and P. Ray, *Physical Review E* **75**, 1 (2007).
 - [7] J. Bakke and A. Hansen, *Physical Review Letters* **100**, 1 (2008).
 - [8] J. Pelletier, *Physical Review Letters* **78**, 2672 (1997).
 - [9] H. J. Catrakis and P. E. Dimotakis, *Physical Review Letters* **77**, 3795 (1996).
 - [10] J. Kondev and G. Huber, *Physical Review Letters* **86**, 5890 (2001).
 - [11] M. Isichenko and J. Kalda, *Journal of Nonlinear Science* **1**, 375 (1991).
 - [12] D. Bernard, G. Boffetta, A. Celani, and G. Falkovich, *Physical Review Letters* **98**, 1 (2007).
 - [13] B. B. Mandelbrot, *The Fractal Geometry of Nature* (Freeman, New York, 1982).
 - [14] M. B. Isichenko, *Review of Modern Physics* **64**, 961 (1992).
 - [15] B. Mandelbrot, *Science* **156**, 636 (1967).
 - [16] J. Kalda, *Europhysics Letters* **84**, 46003 (6pp) (2008).
 - [17] A. Weinrib, *Physical Review B* **29**, 387 (1984).
 - [18] J. M. Ziman, *Journal of Physics C* **1**, 1532 (1968).
 - [19] A. Weinrib, *Physical Review B* **26**, 1352 (1982).
 - [20] J. Kalda, arXiv:0804.1911v1 (2008).
 - [21] J. Kalda, *Physical Review E* **64**, 20101 (2001).

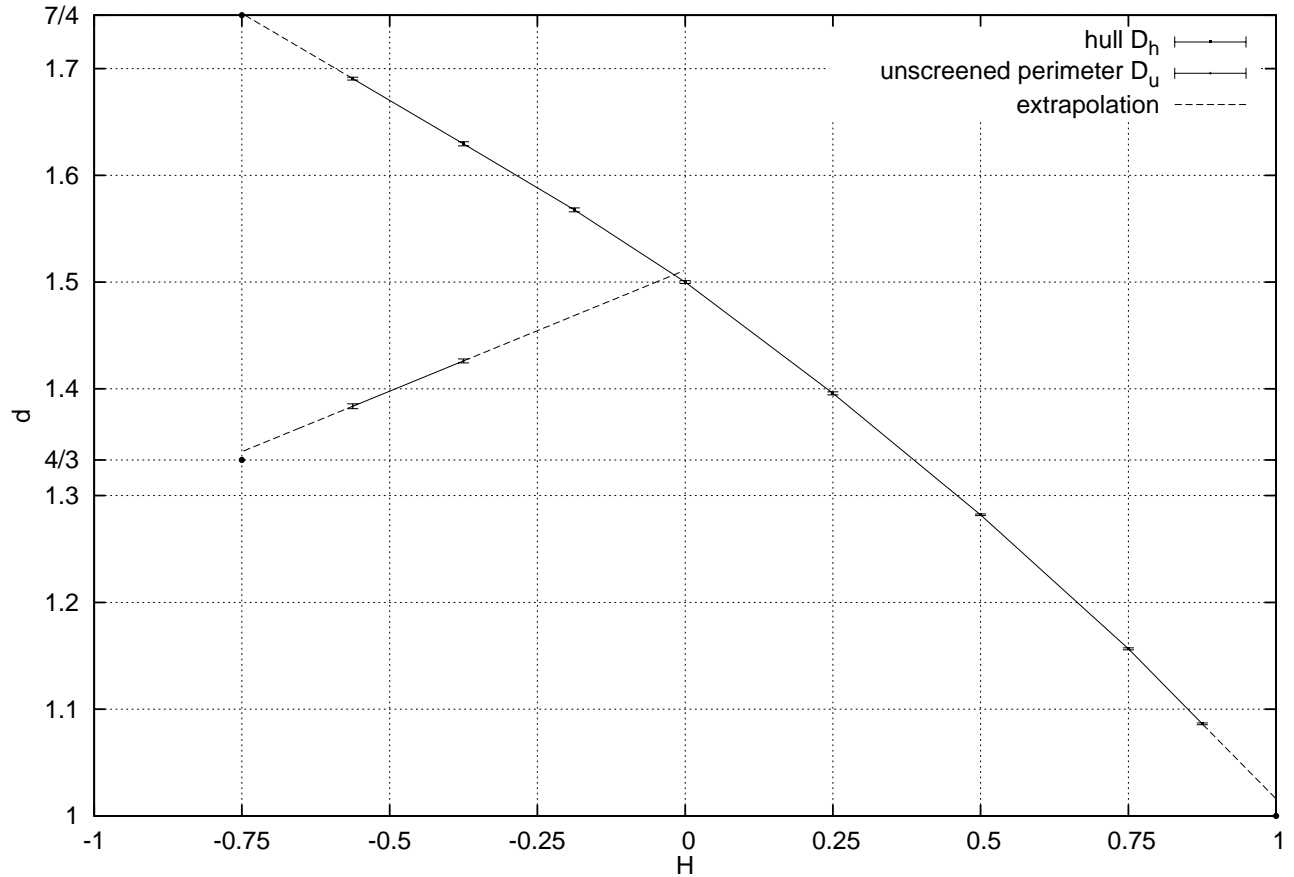


Figure 13: Scaling exponents of the hull and the unscreened perimeter as functions of the Hurst exponent H . Data points for the positive side of D_u are not plotted as to avoid clutter.

H	D_h	D_u
1.0000		
0.8750	1.0862 ± 0.0008	1.0862 ± 0.0022
0.7500	1.1565 ± 0.0010	1.1565 ± 0.0011
0.5000	1.2820 ± 0.0008	1.2820 ± 0.0011
0.2500	1.3958 ± 0.0014	
0.0000	1.5000 ± 0.0013	
-0.1875	1.5676 ± 0.0018	
-0.3750	1.6295 ± 0.0019	1.4261 ± 0.0018
-0.5625	1.6906 ± 0.0014	1.3837 ± 0.0023
-0.7500		

Table I: Numeric results for the hull and the unscreened perimeter (0.95 confidence).

- [22] M. Rajabpour and S. Vaez Allaei, *Physical Review E* **80**, 1 (2009).
 [23] a. Saberi, H. Dashti-Naserabadi, and S. Rouhani, *Physical Review E* **82**, 2 (2010).
 [24] M. Nezhadhighi and M. Rajabpour, *Physical Review*

- E* **83**, 1 (2011).
 [25] S. B. Ramisetti, C. Campañá, G. Ancaux, J.-F. Molinari, M. H. Müser, and M. O. Robbins, *Journal of Physics: Condensed Matter* **23**, 215004 (2011).